Available online at www.sciencedirect.com

SciVerse ScienceDirect

Ceramics International 38 (2012) 4363–4367

CERAMICS INTERNATIONAL

www.elsevier.com/locate/ceramint

Short communication

Mechanical and dielectric properties of gelcasted Si_3N_4 porous ceramic using $CaHPO_4$ as an additive

Xiaoming Duan [a,b], Dechang Jia [b,*], Jie Deng [b], Zhihua Yang [b], Yu Zhou [b]

[a] Key Laboratory of Metal Precision Processing, Harbin Institute of Technology, Harbin 150001, China
[b] Institute for Advanced Ceramics, Harbin Institute of Technology, Harbin 150001, China

Received 6 August 2011; received in revised form 13 December 2011; accepted 3 January 2012
Available online 11 January 2012

Abstract

The phase composition, relative density, mechanical properties and dielectric properties of silicon nitride porous ceramics with different content of $CaHPO_4$ as an additive prepared by gelcasting method were investigated. The addition of $CaHPO_4$ can improve the sintering ability and the phase transformation from α-Si_3N_4 to β-Si_3N_4, so the relative density and β-Si_3N_4 content both increase with the increase of $CaHPO_4$ content. As a result, when the $CaHPO_4$ addition content is 15 wt.%, the flexural strength, elastic modulus, fracture toughness of Si_3N_4 ceramic reach to 365.1 MPa, 107.9 GPa and 3.82 MPa $m^{1/2}$, respectively. The dielectric constant of Si_3N_4 ceramics increases with the increase of $CaHPO_4$ addition content due to the increase of relative density and the relative content of β-Si_3N_4.

Keywords: C. Mechanical properties; C. Dielectric properties; D. Si_3N_4; $CaHPO_4$

1. Introduction

Si_3N_4 ceramic is a kind of material which has received much attraction for its low density, high strength, high fracture toughness, good oxidation resistance, good wave transparent property and superior high temperature performance [1,2], thus is widely used in various areas such as heat exchangers, turbines and automotive engine components, valves and cam roller followers for gasoline and diesel engines and radomes on missiles. Recently, many researches have been focusing on the Si_3N_4 ceramic with a certain volume content of pores serving as the wave transparent window materials. [3]

There are two types of silicon nitride crystals (α-Si_3N_4, β-Si_3N_4) which are now widely used. The mechanical properties of β-Si_3N_4 are higher than that of α-Si_3N_4, while the dielectric properties of α-Si_3N_4 are better. The α-Si_3N_4 can be transform to β-Si_3N_4 during the sintering process with high temperature (1750–1900 °C), and the phase transformation process of Si_3N_4 is carried out by liquid phases.

Phosphate with high temperature thermostability, high strength, excellent dielectric properties and oxidation resistance can be used as advanced wave-transparent materials. In addition, phosphate can also serve as an inorganic chemical binder, which helps the densification of ceramic materials and the improvements of composite performances.

Gelcasting is an attractive new ceramic forming process that is used in manufacturing high-quality and complex-shaped ceramic parts for various industries. Principal advantages include near-net-shape forming, high green density and low organic levels in the dried green bodies. Many studies have been done to promote the gelcasting process, and a wide variety of ceramic materials have been prepared using gelcasting process including Si_3N_4, SiC, Al_2O_3 and ZrO_2 [4–17].

In the present work, the effects of $CaHPO_4$ content on phase compositions, mechanical properties and dielectric properties of Si_3N_4 ceramic prepared by gelcasting method are investigated, and Si_3N_4 ceramic with good mechanical properties and dielectric characteristic is expected to fabricate.

2. Experimental procedure

2.1. Materials processing

Commercial α-Si_3N_4 powder (mean particle size: 0.77 μm, α phase content: 94 vol.%,), $CaHPO_4$ (mean particle size: 70.96 μm, 98% purity) as the sintering additives, polyacrylic

* Corresponding author at: Institute for Advanced Ceramics, Harbin Institute of Technology, P.O. Box 433, Harbin 150001, China. Tel.: +86 451 86418792; fax: +86 451 86414291.
E-mail address: dechangj@gmail.com (D. Jia).

0272-8842/$36.00
doi:10.1016/j.ceramint.2012.01.006

acid as dispersing agent, agarose as gelatinizing agent were used as starting materials in the study. The dicalcium phosphate and silicon nitride powders were mixed by the designed ratios (the $CaHPO_4$ contents are 0 wt.%, 5 wt.%, 10 wt.% and 15 wt.%, respectively) in the deionized water. The polyacrylic acid was added as dispersing agent with 0.3 wt.% solid content, and the ammonia aqueous solution was also added to adjust the pH value to 7.5. The above raw materials were mixed by ball-milling with silicon nitride balls for 24 h, and the composite suspension with 40 vol.% solid contents was made. The 3.0 wt.% agarose solution was prepared at 95 °C in order to fully dissolve agarose in water, and then cooled to 60 °C. The composite suspension and agarose solution were mixed at 60 °C by ball-milling for 2 h. The next step was to pour the mixture solution into a stainless steel mould with a diameter of 58 mm and a height of 8 mm, and they were put into a refrigerator to condense into solid. The sample was dried at room temperature under controlled humidity until the green body contraction is over, and then reduced the humidity in the ventilation drying. The dried green body was heated to 500 °C with a ramp rate of 2 °C/min and held for 2 h to remove the agarose in an electric resistance furnace. Then the green body was embedded in the Si_3N_4 powder in a graphite crucible and sintered at 1650 °C for 1 h in 1 atm N_2 atmosphere.

2.2. Materials characterization

X-ray diffraction (XRD) was carried out using Cu Kα radiation to determine the phase composition. FTIR measurements were performed with a Magna-IR560E spectrometer in the range of 400–1400 cm^{-1} using the KBr pellet technique. The density of the specimen was determined by the Archimedes method, and the theoretical density was calculated according to the rule of mixture. Flexural strength and elastic modulus were measured on bar specimens of 3 mm × 4 mm × 36 mm using a three-point bend fixture with a span of 30 mm and a cross-head speed of 0.5 mm/min. Fracture toughness measurements were performed on single-edge-notched beams (2 mm × 4 mm × 20 mm) with a span of 16 mm at a cross-head speed of 0.05 mm/min, and a half-thickness notch was made using a 0.1 mm thick diamond wafer blade. The microstructure of fracture surfaces were observed by scanning electron microscopy (SEM, FEI Sirion) after being sputtered with gold film. Permittivity of the specimens with a size of ∅18.0 mm × 1.8 mm was recorded in the frequency range of 21–27 GHz at room temperature by RF impedance/material analyzer (Model 4291B, Agilent, USA).

3. Results and discussion

Table 1 shows the relative density and linear shrinkage of the Si_3N_4 ceramic as a function of $CaHPO_4$ addition content. The green bodies with various $CaHPO_4$ addition content have almost the same relative density, while the relative density of sintered ceramics increase significantly with the increase of $CaHPO_4$ addition content, as well as the linear shrinkage. It could be explained by that $CaHPO_4$ used as sintering aids will form liquid phase and promote the rearrangement of grains and the densification of ceramics.

Table 1
Relative density and linear shrinkage of Si_3N_4 ceramic composites as a function of $CaHPO_4$ addition content.

$CaHPO_4$ addition content (wt.%)	Relative density of green body (%)	Relative density of sintering ceramics (%)	Linear shrinkage (%)
0	41.4	46.3	4.33
5	43.1	56.7	11.8
10	43.7	60.2	14.1
15	42.7	72.1	16.8

Table 2
β-Si_3N_4 content of the Si_3N_4 porous ceramics with different $CaHPO_4$ addition content.

$CaHPO_4$ addition content (wt.%)	Relative contents of β-Si_3N_4 (%)
0	49.3
5	67.7
10	85.2
15	89.9

Fig. 1 shows the XRD patterns of ceramics with different $CaHPO_4$ addition content. It could be observed that β-Si_3N_4 and α-Si_3N_4 phases both exist in the sintered samples, and the relative content of β-Si_3N_4 increases obviously with the increase of $CaHPO_4$ addition content.

The volume fraction of β-Si_3N_4 was calculated according to the formula proposed by Hwang [18] by measuring the intensities of (1 0 1), (2 1 0) peaks of β phase and the (1 0 2), (2 1 0) peaks of α phase:

$$\beta\% = \frac{I_{\beta(1\,0\,1)} + I_{\beta(2\,1\,0)}}{[I_{\alpha(1\,0\,2)} + I_{\alpha(2\,1\,0)}] + [I_{\beta(1\,0\,1)} + I_{\beta(2\,1\,0)}]} \times 100\% \quad (1)$$

where $I_{\alpha(1\,0\,2)}$ and $I_{\alpha(2\,1\,0)}$ denote the intensities of (1 0 2) and (2 1 0) diffraction planes of α-Si_3N_4, and $I_{\beta(1\,0\,1)}$ and $I_{\beta(2\,1\,0)}$ denote the intensities of (1 0 1) and (2 1 0) planes of β-Si_3N_4, respectively.

Table 2 shows the calculated results according to Fig. 1 and Eq. (1). The relative content of β-Si_3N_4 increases significantly

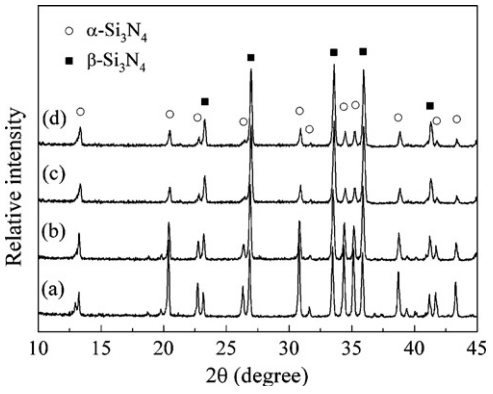

Fig. 1. XRD patterns of the Si_3N_4 porous ceramics with different $CaHPO_4$ addition content. (a) 0 wt.%, (b) 5 wt.%, (c) 10 wt.%, and (d) 15 wt.%.

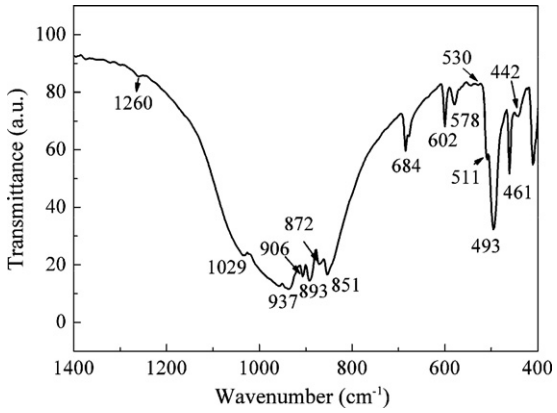

Fig. 2. FTIR spectra of the as-prepared Si_3N_4 porous ceramics.

with the increase of $CaHPO_4$ addition content, and when the $CaHPO_4$ addition content increases to 15 wt.%, the relative content of β-Si_3N_4 reaches to 89.9%.

For determination the constitution of composites, the combination of X-ray diffraction and the Fourier transform infrared spectroscopy (FTIR) have been proved to be suitable methods. With the help of vibrational spectroscopy, good crystalline, poor crystalline, amorphous inorganic components and organic substances can be identified. Fig. 2 shows the FTIR spectrum of Si_3N_4 ceramic with 15 wt.% $CaHPO_4$ addition content. The absorption peaks located at 602 cm^{-1}, 1029 cm^{-1} correspond to PO_4^{3-} ions, 461 cm^{-1}, 493 cm^{-1}, 511 cm^{-1}, 530 cm^{-1} correspond to $P_2O_7^{2-}$ ions, 937 cm^{-1} correspond to Si–N bands, 578 cm^{-1} correspond to Si–O bands. It can be concluded that phosphate or pyrophosphate exist in the ceramic, but they are difficult to be identified from XRD patterns because of their relative low contents.

Fig. 3 shows the SEM fractographs of the Si_3N_4 ceramics with different $CaHPO_4$ addition content. With the increase of the $CaHPO_4$ addition content, the porosity of the ceramics decreases, while the amount of elongated β-Si_3N_4 columnar grains increases. As a sintering additive, $CaHPO_4$ promotes the densification of the ceramics, the phase transformation from α-Si_3N_4 to β-Si_3N_4 as well as the growth of elongated β-Si_3N_4 columnar grains.

Table 3 shows the mechanical properties of Si_3N_4 ceramics as a function of $CaHPO_4$ addition content. With the increase of $CaHPO_4$ addition content, the flexural strength, elastic modulus and fracture toughness of ceramics increase, which have the same trends of relative density and β-Si_3N_4 content. The strengths of materials are mainly affected by the phase compositions and the porosities, and they can be calculated by the following equations:

$$\sigma = \sum \sigma_i v_i \tag{2}$$

where σ denotes the strength of composite material, σ_i denotes the strength of the i-th phase in the composite and the v_i denotes

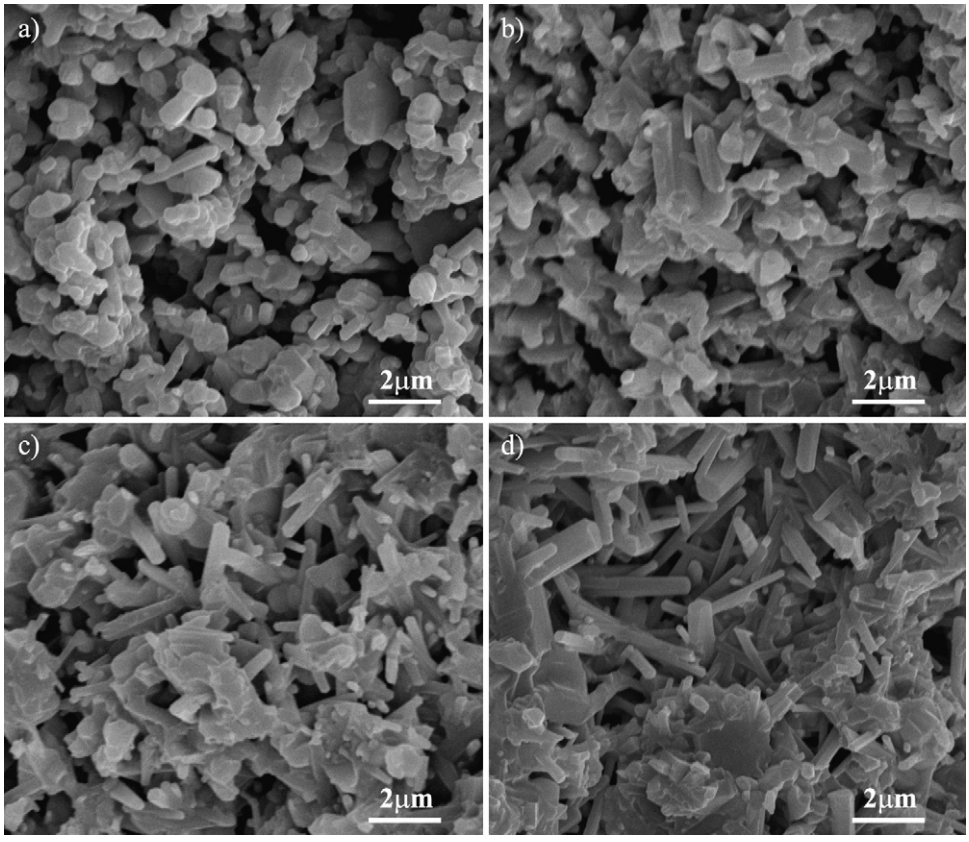

Fig. 3. SEM fractographs of the as-prepared Si_3N_4 porous ceramics with $CaHPO_4$ addition. (a) 0 wt.%, (b) 5 wt.%, (c) 10 wt.%, and (d) 15 wt.%.

Table 3
Mechanical properties of the as-prepared Si_3N_4 porous ceramics as a function of $CaHPO_4$ addition content.

$CaHPO_4$ addition content (wt.%)	Flexural strength (MPa)	Elastic modulus (GPa)	Fracture toughness (MPa $m^{1/2}$)
0	42.1 ± 5.1	25.3 ± 0.6	0.44 ± 0.02
5	180.2 ± 13.7	72.1 ± 0.8	2.00 ± 0.08
10	202.2 ± 22.2	85.7 ± 4.4	2.67 ± 0.24
15	365.1 ± 33.4	107.9 ± 4.6	3.83 ± 0.82

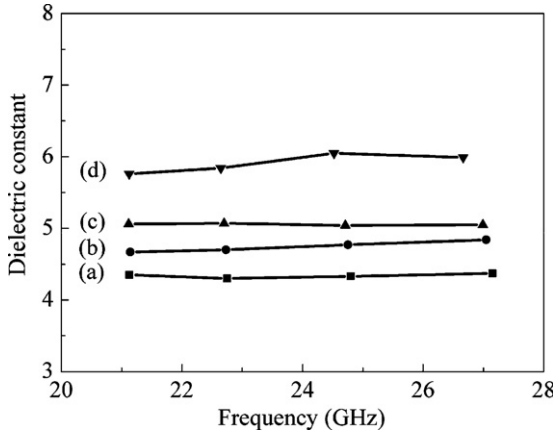

Fig. 4. Dielectric constant of the as-prepared Si_3N_4 porous ceramic as a function of $CaHPO_4$ addition content. (a) 0 wt.%, (b) 5 wt.%, (c) 10 wt.%, and (d) 15 wt.%.

the volume percentage of the *i*-th phase. Since the strength of β-Si_3N_4 is much higher than that of α-Si_3N_4, thus the strength increase of composite ceramics could be explained by both the increase of β-Si_3N_4 contents and the decrease of porosities caused by the content increase of $CaHPO_4$.

Besides mechanical properties, dielectric constant is also an important performance parameter for wave transparent applications. Fig. 4 shows the dielectric constant of the as-prepared Si_3N_4 ceramics as a function of $CaHPO_4$ addition content.

The density and phase composition are the main factors influencing the dielectric constant of the ceramics. The dielectric constant increases with the relative density. XRD patterns prove that both of α-Si_3N_4 and β-Si_3N_4 exist in the ceramics and it should be noted that the dielectric constant of β-Si_3N_4 phase ($\varepsilon = 7.9$) is higher than that of α-Si_3N_4 phase ($\varepsilon = 5.6$). According to the rule of mixture ($\ln \varepsilon = V_1 \ln \varepsilon_1 + V_2 \ln \varepsilon_2$) [19,20] the ceramics has higher dielectric constant with higher β-Si_3N_4 phase content. So with the $CaHPO_4$ addition content increasing, the relative density and β-Si_3N_4 phase content increase, leading to a corresponding increase in the dielectric constant.

4. Conclusions

Si_3N_4 porous ceramics were successfully fabricated by gelcasting method using $CaHPO_4$ as the additive.

(1) With the increase of $CaHPO_4$ addition content, the relative density and the relative content of β-Si_3N_4 in ceramics increase, which proves that the $CaHPO_4$ can promote the densification of ceramics, phase transformation from α-Si_3N_4 to β-Si_3N_4 as well as the development of elongated columnar β-Si_3N_4 grains.
(2) The flexural strength, elastic modulus and fracture toughness of Si_3N_4 ceramics increase with the increase of $CaHPO_4$ addition contents, and they reach to 365.1 MPa, 107.9 GPa, 3.82 MPa $m^{1/2}$ when the $CaHPO_4$ content is added to 15 wt.%.
(3) The dielectric constant of Si_3N_4 ceramics increase with the increase of $CaHPO_4$ addition content because of the increase of relative density and the relative content of β-Si_3N_4.

Acknowledgements

This work was supported by Yangtze Scholars Program in China (2009); National Natural Science Foundation of China (NSFC, 51021002).

References

[1] X.J. Liu, Z.Y. Huang, X.P. Pu, et al., Influence of planetary high-energy ball milling on microstructure and mechanical properties of silicon nitride ceramics, J. Am. Ceram. Soc. 88 (2005) 1323–1326.
[2] C.J. Lee, D.J. Kim, Effect of α-Si_3N_4 particle size on the microstructure evolution of Si_3N_4 ceramics, J. Am. Ceram. Soc. 82 (1999) 753–756.
[3] D.G. Paqutte, Method of making a radar transparent window material operable above 2000 °C, US Patent 5,627,542 (1997).
[4] Santacruz, M.I. Nieto, R. Moreno, Alumina bodies with near-to-theoretical density by aqueous gelcasting using concentrated agarose solutions, Ceram. Int. 31 (2005) 439–445.
[5] J.Q. Dai, Y. Huang, Z.P. Xie, et al., Effect of acid cleaning and calcination on rheological properties of concentrated aqueous suspensions of silicon nitride powder, J. Am. Ceram. Soc. 85 (2002) 293–298.
[6] M.H. Bocanegra-Bernal, B. Matovic, Dense and near-net-shape fabrication of Si_3N_4 ceramics, Mater. Sci. Eng. A 500 (2009) 130–149.
[7] M.J. Dong, X.J. Mao, Z. Zhang, et al., Gelcasting of SiC using epoxy resin as gel former, Ceram. Int. 35 (2009) 1363–1366.
[8] J.L. Yu, H.J. Wang, Effect of monomer content on physical properties of silicon nitride ceramic green body prepared by gelcasting, Ceram. Int. 35 (2009) 1039–1044.
[9] J.M. Tulliani, C. Bartuli, E. Bemporad, et al., Preparation and mechanical characterization of dense and porous zirconia produced by gelcasting with gelatin as a gelling agent, Ceram. Int. 35 (2009) 2481–2491.
[10] C. Zhang, X. Huang, Y. Yin, et al., Preparation of boron carbide aluminum composites by non-aqueous gelcasting, Ceram. Int. 35 (2009) 2255–2259.
[11] C. Tallon, D. Jach, R. Moreno, M. Nieto, G. Rokicki, Gelcasting of alumina suspensions containing nanoparticles with glycerol monoacrylate, J. Eur. Ceram. Soc. 29 (2009) 875–880.
[12] M. Mamoru, P. Guenter, Recent progress in silicon nitride and silicon carbide ceramics, MRS Bull. 20 (1995) 19–20.
[13] Y. Huang, L.J. Zhou, Q. Tang, et al., Water-based gelcasting of surface-coated silicon nitride powder, J. Am. Ceram. Soc. 84 (2001) 701–707.
[14] C. Kawai, T. Matsuura, A. Yamakawa, Separation–permeation performance of porous Si_3N_4 ceramics composed of columnar β-Si_3N_4 grains as membrane filters for microfiltration, J. Mater. Sci. 34 (1999) 893–896.
[15] J.F. Yang, T. Ohji, S. Kanzaki, et al., Microstructure and mechanical properties of silicon nitride ceramics with controlled porosity, J. Am. Ceram. Soc. 85 (2002) 1512–1516.

[16] T. Giuliano, Gelcasting ceramics: a review, Am. Ceram. Soc. Bull. 82 (2003) 43–47.
[17] M.A. Omatete, R.A. Janney, Strehlow, Gelcasting—a new ceramic forming process, Am. Ceram. Soc. Bull. 70 (1991) 1641–1649.
[18] J. Hwang, R.A. Newman, Silicon nitride ceramics with celsian as an additive, J. Mater. Sci. 31 (1996) 2521–2526.
[19] K. Lichtenecker, Dielectric constants of cubic ionic compounds, Physik Zeits. 27 (1926) 833–835.
[20] J.Q. Li, F. Luo, M.D. Zhu, et al., Influence of phase formation on dielectric properties of Si_3N_4 ceramics, J. Am. Ceram. Soc. 90 (2007) 1950–1952.